Deformation potential constants of biaxially tensile stressed Ge epitaxial films on Si(100)

Jifeng Liu, Douglas D. Cannon, Kazumi Wada,* Yasuhiko Ishikawa, David T. Danielson, Samerkhae Jongthammanurak, Jurgen Michel, and Lionel C. Kimerling

Department of Materials Science and Engineering, Massachusetts Institute of Technology, Cambridge, Massachusetts 02139, USA

(Received 24 April 2004; published 14 October 2004)

The deformation potential constants at the Γ point of Ge epitaxial films on Si(100) were determined by a combination of x-ray diffraction and photoreflectance measurements. The in-plane tensile strain in the Ge thin films was engineered by growth at different temperatures in ultrahigh vacuum chemical vapor deposition and by backside silicidation. Photoreflectance measurements and data analysis give the direct band gaps from the maxima of the light- and the heavy-hole bands to the bottom of Γ valley, namely, $E_g^{\Gamma}(lh)$ and $E_g^{\Gamma}(hh)$. From the relationship between the direct band gap and the in-plane strain measured by x-ray diffraction, the dilational deformation potential of the direct band gap of Ge a, and the shear deformation potential of the valence band b were determined to be -8.97 ± 0.16 eV and -1.88 ± 0.12 eV, respectively. These basic constants of Ge are very important for the design of strain-engineered devices based on epitaxial Ge.

DOI: 10.1103/PhysRevB.70.155309 PACS number(s): 73.61.Cw, 71.70.Fk

I. INTRODUCTION

In recent years, there has been an extensive study concerning the effect of strain on the band structure of semiconductors due to potential applications in electronic and optoelectronic devices. Strained III-V semiconductor quantum well structures have been applied to low threshold laser diodes.[1] Strained Si on the SiGe alloy layer has been developed for high-frequency complimentary metal-oxide-semiconductor devices.[2–4] In our previous studies, we have shown that tensile strained Ge films epitaxially grown on Si have higher absorption coefficients in the near-infrared regime than bulk Ge due to the tensile strain induced direct band-gap shrinkage, and are good candidates for near-infrared photodetectors in telecommunications.[5–7] However, due to the fact that Ge is usually only considered as an indirect band-gap material, there have been relatively few studies in the literature on the direct band-gap of Ge, which is crucial for its optoelectronic properties. Furthermore, due to the brittleness of Ge bulk material all the previous experimental studies on the effect of stress/strain on the band structure of Ge have been based on uniaxial or hydrostatic compression tests,[8–17] and there have been no experimental reports on the effect of biaxial tensile stress on the band structure of Ge films, which is indispensable knowledge to engineer strained Ge for epitaxy-based optoelectronic devices. In this paper, we study the effect of biaxial tensile stress on the direct band gap of Ge and derive the dilational and shear deformation potential constants a and b, for the direct band gap at room temperature. These parameters are important for predicting the effect of strain on the optoelectronic properties of Ge, especially the biaxially stressed electronic and optoelectronic devices based on epitaxial Ge.

II. EXPERIMENT

Epitaxial Ge films were deposited by a two-step ultrahigh vacuum chemical vapor deposition (UHV-CVD) on double side polished, 4-in. B doped p^+Si(100) substrates with a resistivity of 0.001–0.002 Ω cm. Low-temperature buffer layers of ~50 nm were deposited at 335 °C to achieve planar growth, followed by high-temperature depositions at 600, 650, 700 and 800 °C, respectively, to obtain different tensile strain in the Ge epitaxial films. Details of this growth method were reported earlier.[18] The film thickness ranges from 1.3 μm to 1.7 μm, as determined by Rutherford backscattering. The surfaces of the Ge epitaxial films are very smooth, with ~1 nm root-mean-square roughness as revealed by atomic force microscopy (AFM). The threading dislocation density of the as-grown films is $\sim 8\times10^8/\mathrm{cm}^2$, as determined by transmission electron microscopy. The Ge films are nominally undoped, and the secondary-ion mass spectrometry shows a residual B concentration of $\sim10^{14}/\mathrm{cm}^3$, most likely due to the B diffusion from the p^+ Si substrate during the growth. Since the film thickness is far greater than the critical thickness for pseudomorphic growth of Ge on Si (about a few monolayers),[19] the films are almost fully relaxed at the growth temperature (≥600 °C). Upon cooling to room temperature, tensile strain is accumulated in the Ge films due to the larger thermal expansion coefficient of the Ge film compared with the Si substrate.[5,6] In UHV-CVD deposition, Ge films are naturally deposited on both sides of the double side polished Si(100) wafers, which provides a nearly perfect biaxial stress state in the Ge films. To further increase the strain in the front side Ge film, the backside Ge was etched off by H_2O_2 followed by the deposition of Ti films of 1.2–1.5 μm on the backside of the wafer and rapid thermal annealing to form 3.0–3.8 μm of C54-$TiSi_2$. The large tensile stress (~2 GPa) in the C54-$TiSi_2$ film induces a slight bending of the wafer toward the backside and further enhances the strain in the frontside Ge film by ~0.05%. Details of this backside silicidation process have been reported elsewhere.[7] Samples $\sim1\times1$ cm^2 in sizes were cut from the wafer for x-ray diffraction (XRD) and photoreflectance (PR) measurements. The XRD was carried out on a Rigaku 250 mm high-resolution Bragg Brettano diffractometer with Cu K_α irradiation. The strain in the epitaxial Ge films was measured by comparing the Ge(400) and (422)

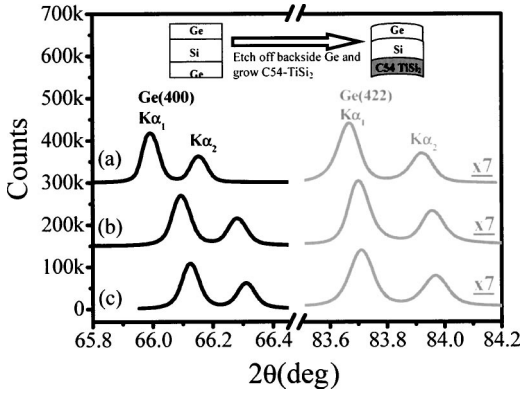

FIG. 1. Ge(400) (black lines) and (422) (gray lines) x-ray diffraction peaks of (a) bulk Ge(100) wafer, (b) Ge on Si grown at 700°C, and (c) Ge/Si/3.0 μm C54-$TiSi_2$. The intensity of the Ge(422) peaks are magnified by a factor of 7. The shift of the peaks to higher 2θ angles in (b) and (c) compared with (a) indicates the existence of tensile stress in the Ge epitaxial films on Si. The inset of the figure schematically shows the backside silicidation process.

peak positions in θ-2θ XRD step scans of the Ge thin films with a lightly doped *n*-type 2-in. Ge(100) single-crystal wafer. The XRD step scan was carried out at 0.002° per step with a data collection time of 2 sec/step. Before each scan of Ge/Si(100) samples, the diffractometer was calibrated in such a way that the $K_{\alpha 1}$ diffraction peak of Si(400) from the substrate was maximized and at its theoretical position (θ = 34.566°). PR measurement was employed to determine the direct band gaps of the Ge films. A 488 nm Ar laser with a power of 10 mW was used as the pump source and was modulated at a frequency of 201 Hz by a chopper to achieve electric-field modulation on the sample surface. A halogen lamp with scanning monochrometer was used as the light source for reflectivity measurements. The monochrometer scanned at 0.5 nm/step with a Rayleigh resolution of 16 nm and the data collection time was 60 sec/step. Data fitting with the third derivative spectroscopy model[20] and the generalized theory of Franz-Keldysh oscillations[21–23] give the direct band gaps from the maximum of the light- and the heavy-hole bands to the bottom of Γ valley, namely, $E_g^{\Gamma}(lh)$ and $E_g^{\Gamma}(hh)$. The dilational deformation potential of the direct bandgap of Ge *a*, and the shear deformation potential of the valence band *b*, were derived from the direct band gap versus strain relationship.

III. RESULTS AND DISCUSSIONS

The strain in the Ge epitaxial films on Si was determined by XRD. As representative examples, Fig. 1 shows the Ge(400) and (422) diffraction peaks of the bulk Ge(100) sample, the Ge/Si sample grown at 700°C and the Ge/Si/3.0 μm C54-$TiSi_2$ sample. The (400) peaks of Ge epitaxial films [Figs. 1(b) and 1(c)] shift significantly to higher 2θ angles with respect to the bulk Ge sample [Fig.1(a)], indicating the existence of tensile stress in the Ge films. The $K_{\alpha 1}$ peak positions were determined by the parabolic top method and used to calculate the lattice spacing of Ge(400) and (422) planes. The lattice parameter determined for bulk Ge is 0.565 80 nm, highly consistent with the value reported in literature[24] and indicating the accuracy of our XRD measurements. For the Ge epitaxial films on Si(100), the in-plane strain $\varepsilon_{\parallel}$ and the strain perpendicular to the film $\varepsilon_{\perp}$ can be determined from the XRD data by

$$\varepsilon_{\perp} = \varepsilon_{400},$$

$$\varepsilon_{\parallel} = 3\varepsilon_{422} - 2\varepsilon_{400}. \quad (1)$$

Here ε_{400} and ε_{422} are the strain in the [400] and [422] directions of the Ge film, respectively. We also carried out (422) scans of the Ge epitaxial film in two orthogonal directions, i.e., [011] and $[01\bar{1}]$, to check any strain relaxation anisotropy. Within the range of experimental error, no anisotropy in the strain relaxation was observed. Therefore, $\varepsilon_{\parallel}$ is isotropic in the plane of the Ge film. Table I summarizes $\varepsilon_{\parallel}$

TABLE I. Strain and direct band gaps of the epitaxial Ge films on Si(100) used in this study.

Ge growth temperature (°C)	Backside C54-$TiSi_2$ thickness (μm)	ε_{400}(%)	ε_{422}(%)	$\varepsilon_{\parallel}$(%)	$\varepsilon_{\perp}$(%)	$\varepsilon_{\parallel}/\varepsilon_{\perp}$	$E_g^{\Gamma}(lh)$ (eV)	$E_g^{\Gamma}(hh)$ (eV)
600	N/A	−0.0977 ±0.0013	−0.0213 ±0.0010	0.131 ±0.004	−0.0977 ±0.0013	−1.34 ±0.06	0.7815 ±0.0005	0.7903 ±0.0006
650	N/A	−0.1298 ±0.0015	−0.0298 ±0.0010	0.170 ±0.004	−0.1298 ±0.0015	−1.31 ±0.05	0.7758 ±0.0006	0.7873 ±0.0006
700	N/A	−0.1390 ±0.0015	−0.0318 ±0.0011	0.183 ±0.004	−0.139 ±0.0015	−1.32 ±0.04	0.7743 ±0.0005	0.7863 ±0.0005
800	N/A	−0.1452 ±0.0014	−0.0314 ±0.0012	0.196 ±0.005	−0.1452 ±0.0014	−1.35 ±0.05	0.7727 ±0.0004	0.7852 ±0.0005
800	3.0	−0.1805 ±0.0015	−0.0403 ±0.0010	0.240 ±0.004	−0.1805 ±0.0015	−1.33 ±0.03	0.7656 ±0.0007	0.7815 ±0.0005
800	3.8	−0.1846 ±0.0015	−0.0394 ±0.0012	0.251 ±0.005	−0.1846 ±0.0015	−1.36 ±0.03	0.7640 ±0.0007	0.7805 ±0.0005

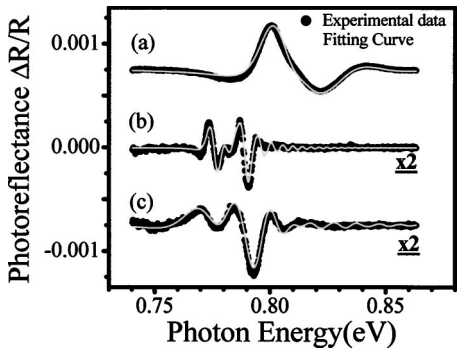

FIG. 2. Photoreflectance ($\Delta R/R$) spectra of (a) bulk Ge(100) wafer, (b) Ge/Si grown at 700°C, and (c) Ge/Si/3.0 μm C54-$TiSi_2$ sample. The spectrum of the bulk Ge sample was fitted with the conventional third derivative model, while those of Ge/Si and Ge/Si/C54-$TiSi_2$ samples were fit with the generalized theory of Franz-Keldysh oscillations. The fitting yields the direct bandgaps of the bulk Ge and $E_g^\Gamma(lh)$ and $E_g^\Gamma(hh)$ of Ge epitaxial films.

and $\varepsilon_\perp$ of each sample. In theory, we have $\varepsilon_\parallel/\varepsilon_\perp = -C_{11}/(2C_{12}) = -1.33$ under biaxial stress, using $C_{11} = 128.5$ GPa and $C_{12} = 48.3$ GPa (Ref. 24) for bulk Ge. In our measurements we found $\varepsilon_\parallel/\varepsilon_\perp = -1.33 \pm 0.05\%$ for our Ge epitaxial films grown on Si, which is identical to the bulk Ge value within the experimental error. This result again reflects the accuracy of the strain measurements.

The same samples used in XRD were subjected to PR measurement to establish a one to one correspondence between the direct band gap of Ge and the in-plane strain $\varepsilon_\parallel$. The PR data of the bulk Ge was fit with the conventional third derivative spectroscopy model since the surface electric field in bulk Ge is usually low.[20] The fitting gives $E_g^\Gamma = 0.8005 \pm 0.0007$ eV for the unstressed bulk Ge [Fig. 2(a)], in good agreement with the literature and attesting to the accuracy of our PR measurement system.[24] For the Ge epitaxial films on p^+ Si, however, there is a significant builtin electric field and the third derivative model (low-field approximation) cannot fit the data so well anymore. Therefore, the PR data from Ge epitaxial films on Si were analyzed by the generalized Franz-Keldysh theory developed by Shen *et al.*[21,22] For the fundamental band-gap transitions,

$$\Delta R/R \propto \mathrm{Re}(\delta\varepsilon), \tag{2a}$$

where $\delta\varepsilon$ is the change in the dielectric constant given by

$$\begin{aligned}\delta\varepsilon(E,F_{dc},F_{ac}) &= \varepsilon(E,F_{dc}) - \varepsilon(E,F_{dc}-F_{ac}) \\ &= \Delta\varepsilon(E,F_{dc}) - \Delta\varepsilon(E,F_{dc}-F_{ac}).\end{aligned} \tag{2b}$$

In Eq. (2b), E is the incident photon energy, F_{dc} is the builtin electric field in the intrinsic Ge epitaxial film grown on p^+ Si(100), F_{ac} is the electric field induced by the ac modulation of the chopped pump laser, and

$$\Delta\varepsilon(E,F) = \varepsilon(E,F) - \varepsilon(E,0). \tag{2c}$$

In our case, as the light- and heavy-hole valence bands of Ge become nondegenerate under biaxial stress,[25] the spectrum is the sum of contributions from light- and heavy-hole band transitions, characterized by band gaps $E_g^\Gamma(lh)$ and $E_g^\Gamma(hh)$, respectively. Therefore, we have

$$\begin{aligned}\Delta\varepsilon(E,F) = (1/E^2)\{&B_{lh}(\hbar\Theta_{lh})^{1/2}[G(\eta_{lh}) + iF(\eta_{lh})] \\ &+ B_{hh}(\hbar\Theta_{hh})^{1/2}[G(\eta_{hh}) + iF(\eta_{hh})]\},\end{aligned} \tag{3a}$$

where B_{lh} and B_{hh} are constants for light- and heavy-hole transitions, respectively; $G(\eta)$and $F(\eta)$ are electro-optic functions given in Refs. 21–23, and

$$\eta_{lh} = [E_g^\Gamma(lh) - E - i\gamma_{lh}]/\hbar\Theta_{lh},$$

$$\eta_{hh} = [E_g^\Gamma(hh) - E - i\gamma_{hh}]/\hbar\Theta_{hh}. \tag{3b}$$

In Eq. (3b), γ_{lh} and γ_{hh} are the broadening factors of light- and heavy-hole band transitions, respectively; $\hbar\Theta_{lh}$ and $\hbar\Theta_{hh}$ are the electro-optical energies of light- and heavy-hole band transitions, respectively, given by

$$\hbar\Theta_{lh} = (q^2\hbar^2F^2/2\mu_{lh,\parallel})^{1/3},$$

$$\hbar\Theta_{hh} = (q^2\hbar^2F^2/2\mu_{hh,\parallel})^{1/3}, \tag{3c}$$

where q is the electron charge, $\hbar$ is Planck's constant h divided by 2π, F is the electric field, and $\mu_{lh,\parallel}$ and $\mu_{hh,\parallel}$ are the reduced mass of electron-hole pairs of light and heavy holes in the direction parallel to the electric field F, respectively. With Eqs. (2a)–(3c), we are able to fit the PR spectra of epitaxial Ge films on Si. This model fits the experimental data quite well, with correlation coefficients greater than 0.98, as shown in Figs. 2(b) and 2(c). The derived band gaps $E_g^\Gamma(lh)$ and $E_g^\Gamma(hh)$ are presented in Table I.

One has to be careful when relating the direct band-gap values at the Γ point measured by PR to the strain measured by XRD. X ray is able to penetrate the whole Ge film and the strain measured by XRD is an average over the depth of the film. In PR measurements, however, the probed depth is determined by the carrier diffusion length,[23] which can be smaller than the depth of the films. From the *p-i-n* diode performance of our epitaxial Ge/Si photodetectors, we derived that the carrier mobility and lifetime were 3500 cm^2/V sec and 0.8 ns, respectively, for cyclic annealed Ge films with a threading dislocation density of $\sim 2 \times 10^7/cm^2$.[26] Since the minority carrier lifetime is known to be inversely proportional to the dislocation density in Ge,[27] we estimate the minority carrier lifetime of the Ge epitaxial films used in this study (with a threading dislocation density of $\sim 8 \times 10^8/cm^2$) is ~ 0.02 ns. It is also known that the carrier mobility and diffusivity in Ge at room temperature are relatively insensitive to the dislocation scattering up to a dislocation density in the order of $10^8/cm^2$ (Ref. 28). Actually, the carrier diffusivity parallel to the dislocations, $D_\parallel = 400 \pm 100$ cm^2/sec, is greater than that in dislocation-free Ge (100 cm^2/sec), while the diffusivity perpendicular to the dislocations, $D_\perp = 80 \pm 30$ cm^2/sec, is slightly smaller than that in dislocation-free Ge. Even with the lower limit of $D_\perp$ (50 cm^2/sec), we still get a carrier diffusion length of $L = \sqrt{D\tau} \sim 300$ nm. Note that in our samples the carrier diffusion length should be greater than this value, because in PR measurements the carriers diffuse in the direction perpendicular to the film, which is mostly parallel to the threading

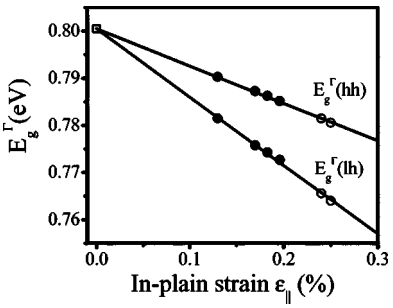

FIG. 3. The direct band gaps of Ge as a function of in-plane strain obtained from PR and XRD measurements. The open square (□) is the data of unstrained bulk Ge(100) single crystal. The solid circles (●) show the band-gap shrinkage of Ge/Si samples grown at different temperatures, while the open circles (○) show further band-gap shrinkage induced by backside silicidation. The black lines show the fitting to the experimental data with Eqs. (4a) and (4b). Deformation potential values $a=-8.97\pm0.16$ eV and $b=-1.88\pm0.12$ eV are derived from the fitting.

dislocations (mostly 90° and 60° dislocations).[18] This means the real diffusivity should be closer to $D_\parallel$ and greater than $D_\perp$. Therefore, we can conclude that the probing depth of PR, determined by the carrier diffusion length, is at least 300 nm. If there were significant surface stress relaxation in the Ge films typically characterized by the formation of a wavy surface or islanding, then the strain in the top 300 nm Ge surface layer would be smaller than that measured by XRD and we would not be able to relate the band gaps measured by PR to the strain measured by XRD. In our case, AFM has confirmed that the surfaces of the Ge epitaxial films used in this study are very smooth, with a root-mean-square roughness of ~1 nm, i.e., there is no sign of surface stress relaxation or islanding in the epitaxial Ge films and the roughness is much smaller than the detection depth (>300 nm) of PR. Therefore, it is safe to state that the strain in the top 300 nm of the Ge film should not be affected by the trivial surface roughness, and that it is valid to establish a one to one correspondence between the direct band gap of Ge and the in-plane strain $\varepsilon_\parallel$ from our experimental results.

The relationship between the direct band gaps $E_g^\Gamma(lh)$and $E_g^\Gamma(hh)$, and the in-plane strain $\varepsilon_\parallel$ is plotted in Fig. 3. The error bars are within the symbols of the data points. According to deformation potential theory, this relationship is given by [12,25]

$$E_g^\Gamma(lh,\varepsilon_\parallel) = E_g^\Gamma(0) + a(\varepsilon_\perp + 2\varepsilon_\parallel) + \Delta_0/2 - 1/4\,\delta E_{100} - 1/2\sqrt{\Delta_0^2 + \Delta_0\delta E_{100} + 9/4(\delta E_{100})^2}, \quad (4a)$$

$$E_g^\Gamma(hh,\varepsilon_\parallel) = E_g^\Gamma(0) + a(\varepsilon_\perp + 2\varepsilon_\parallel) + 1/2\,\delta E_{100}, \quad (4b)$$

where $E_g^\Gamma(lh,\varepsilon_\parallel)$ and $E_g^\Gamma(hh,\varepsilon_\parallel)$ are the band gaps from the maxima of the light- and heavy-hole valence bands to the bottom of Γ valley under an in-plane strain $\varepsilon_\parallel$, respectively. $E_g^\Gamma(0)=0.8005\pm0.0007$ eV is the direct band gap of unstrained bulk Ge at room temperature, as determined in this study; a and b are deformation potential constants of [100] Ge at room temperature; $\delta E_{100}=2b(\varepsilon_\perp-\varepsilon_\parallel)$; and $\Delta_0=0.289$eV from our PR measurement of the split-off band transition of the bulk Ge. By fitting the experimental data in Fig. 3 with Eqs. (4a) and (4b) and [note in Eqs. (4a) and (4b), $\varepsilon_\perp$ can be substituted by $\varepsilon_\perp=-\varepsilon_\parallel/1.33$ as shown in Table I], we obtain $a=-8.97\pm0.16$ eV and $b=-1.88\pm0.12$ eV. The error bars of a and b are determined in the following way: to reflect the effect of the error bars of each data point in Fig. 3 on the uncertainties of a and b, we have written a computer code to generate randomly 10 000 sets of E_g^Γ(lh) and E_g^Γ(hh) vs $\varepsilon_\parallel$ data within their error bars listed in Table I, do a curve fit for each set of data to get a and b, and finally do a statistics on the distribution of a and b due to the variation of the experimental data points within their error bars. The average values of a and b are −8.97 and −1.88 eV, respectively. Ninety percent of the data fall into the range of $a=-8.97\pm0.16$ eV and $b=-1.88\pm0.12$ eV. Therefore, the deformation potential constant data obtained above guarantee 90% confidence. These values are compared with earlier experimental data from literature in Table II. Typically dE_g^Γ/dP (change in direct band gap per unit pressure) instead of a was directly measured from previous experiments and reported in the literature, so we have converted it into a for comparison with our result by the relation:[29]

$$a = -\frac{(C_{11}+2C_{12})}{3}\frac{dE_g^\Gamma}{dP}. \quad (5)$$

All the literature values were measured from either hydrostatic or uniaxial compression tests of single-crystal Ge samples. Looking through Table II, the a value obtained in this work is only consistent with Ref. 12 (uniaxial compression test, room temperature) and Ref. 16 (hydrostatic compression test, room temperature). The value of $|b|$ obtained in this work is consistent with the lower values reported in literature, i.e., Refs. 8–10. As can be seen from Table II, the deformation potential constants reported in literature varied significantly, with the highest reported values greater than

TABLE II. Comparison of the deformation potential constants obtained in this work with the literature.

	This work	Literature	Reference
		−8.0	11
		−9.0±0.4	12
a(eV)	−8.97±0.16	−9.08±0.15	16
		−10.3±0.4	17
		−10.4±0.8	14
		−11.5±0.4	15
		−1.8±0.3	8
		−1.9±0.2 (Al doped Ge)	9
		−2.2±0.2 (In doped Ge)	9
b(eV)	−1.88±0.12	−2.21±0.13	10
		−2.4±0.2	11
		−2.6±0.2	12
		−2.7±0.3	13
		−2.86±0.15	14

the lowest ones by as much as ~50%. This large dispersion may result from the nonuniformity of the stress in the samples, especially in the uniaxial compression tests where the samples tend to bend and deviate from the ideal uniaxial compression. In our samples, the biaxial tensile stress in the Ge epitaxial films was induced by the thermal mismatch between Ge and Si, which gives more uniform stress in the Ge material. While previous measurements sampled a large range of strain up to several percent, the current work has more data points in the small strain regime ($<0.25\%$), which is more consistent with the basic assumptions of deformation potential theory, i.e., the strain Hamiltonian is much less than the spin-orbit Hamiltonian. The XRD diffraction method used in the present study also gives a rather accurate measurement of small strains. Thus, the error bars of the deformation potential constants in this work are smaller than most previous experimental reports. The deformation potential values a and b are obtained for the biaxially tensile stressed Ge. The deformation potential constants obtained in this study are especially suitable for the design of electronic and optoelectronic devices based on epitaxial Ge and SiGe, for these planar devices are exactly in the biaxial stress state.

IV. CONCLUSIONS

The present paper has first reported the direct band gap vs strain relationship of biaxially tensile stressed Ge epitaxial films on Si through a combination of XRD and PR measurements. Deformation potential values $a=-8.97\pm0.16$ eV and $b=-1.88\pm0.12$ eV are derived from this relationship. The uniformity of thermally induced stress in Ge films and the accuracy of x-ray diffraction in determining the small strain improve the preciseness of the measured deformation potential data. These basic constants of Ge are important for the design of strain-engineered optoelectronic and electronic devices based on epitaxial Ge and SiGe.

ACKNOWLEDGMENTS

This work was supported by Pirelli Lab S.p.A. under Contract MIT-Pirelli Alliance agreement dated 9/01/2001.

*Present address: Department of Materials Engineering, Graduate School of Engineering, The University of Tokyo, 7-3-1 Hongo, Bunkyo, Tokyo 113-8656, Japan. URL: http://www.microphotonics.material.t.u-tokyo.ac.jp/

[1] P. J. A. Thijs, L. F. Tiemeijer, P. I. Kuindersma, J. J. M. Binsma, and T. Vandongen, IEEE J. Quantum Electron. **27**, 1426 (1991).
[2] D. K. Nayak, J. C. S. Woo, J. S. Park, K. L. Wang, and K. P. MacWilliams, Appl. Phys. Lett. **62**, 2853 (1993).
[3] J. Welser, J. L. Hoyt, and J. F. Gibbons, IEEE Trans. Electron Devices **15**, 100 (1994).
[4] K. K. Rim, J. L. Hoyt, and J. F. Gibbons, IEEE Trans. Electron Devices **47**, 1406 (2000).
[5] Y. Ishikawa, K. Wada, D. D. Cannon, J. F. Liu, H. C. Luan, and L. C. Kimerling, Appl. Phys. Lett. **82**, 2044 (2003).
[6] D. D. Cannon, J. F. Liu, Y. Ishikawa, K. Wada, D. T. Danielson, S. Jongthammanurak, J. Michel, and L. C. Kimerling, Appl. Phys. Lett. **84**, 906 (2004).
[7] J. F. Liu, D. D. Cannon, K. Wada, Y. Ishikawa, S. Jongthammanurak, D. T. Danielson, J. Michel, and L. C. Kimerling, Appl. Phys. Lett. **84**, 660 (2004).
[8] I. Balslev, Phys. Rev. **143**, 636 (1966).
[9] J. J. Hall, Phys. Rev. **128**, 68 (1962).
[10] J. C. Hensel and K. Suzuki, Phys. Rev. B **9**, 4219 (1974).
[11] I. Balslev, Solid State Commun. **5**, 315 (1967).
[12] F. H. Pollak and M. Cardona, Phys. Rev. **172**, 816 (1968).
[13] A. P. Smith III, M. Cardona, and F. H. Pollak, Bull. Am. Phys. Soc. **12**, 101 (1967).
[14] M. Chandrasekhar and F. H. Pollak, Phys. Rev. B **15**, 2127 (1977).
[15] B. Welber, M. Cardona, Y. F. Tsay, and B. Bendow, Phys. Rev. B **15**, 875 (1977).
[16] A. R. Goñi, K. Syassen, and M. Cardona, Phys. Rev. B **39**, 12 921 (1989).
[17] G. H. Li, A. R. Goñi, K. Syassen, and M. Cardona, Phys. Rev. B **49**, 8017 (1994).
[18] H.-C. Luan, D. R. Lim, K. K. Lee, K. M. Chen, J. G. Sandland, K. Wada, and L. C. Kimerling, Appl. Phys. Lett. **75**, 2909 (1999).
[19] E. A. Fitzgerald, Mater. Sci. Rep. **7**, 87 (1991).
[20] D. E. Aspnes, Surf. Sci. **37**, 418 (1973).
[21] H. Shen and F. H. Pollak, Phys. Rev. B **42**, 7097 (1990).
[22] H. Shen and M. Dutta, J. Appl. Phys. **78**, 2151 (1995).
[23] F. H. Pollak, Surf. Interface Anal. **31**, 938 (2001).
[24] *Physics of Group IV Elements and III-V Compounds*, edited by O. Madelung, Landolt-Börnstein: New Series, Group III, Vol. 17, pt. a (Springer-Verlag, Berlin, 1982); *Semiconductors. Intrinsic Properties of Group IV Elements and III-V, II-V, and I-VII Compounds*, edited by O. Madelung, Landolt-Börnstein, New Series, Group III, Vol. 22 pt. a (Springer-Verlag, Berlin, 1987).
[25] C. G. Van de Walle, Phys. Rev. B **39**, 1871 (1989).
[26] L. Colace, G. Masini, G. Assanto, H. C. Luan, K. Wada, and L. C. Kimerling, Appl. Phys. Lett. **76**, 1231 (2000).
[27] G. K. Wertheim and G. L. Pearson, Phys. Rev. **107**, 694 (1957).
[28] H. F. Matare, *Defect Electronics in Semiconductors* (John Wiley & Sons, New York, 1971).
[29] F. H. Pollak, Semicond. Semimetals **32**, 17 (1990).